*J. Agr. Sci. Tech. (2009) Vol. 11: 377-389*

# An Extended Octagonal Ring Transducer for the Compression Chamber of a Large Square Baler

S. Afzalinia[1]*, and M. Roberge[2]


## ABSTRACT

**An extended octagonal ring (EOR) transducer was designed and developed to measure forces inside the compression chamber of a large square baler in different directions. The transducer was calibrated by applying forces in three directions simultaneously and independently. The sensor revealed excellent linearity along with small cross sensitivities. Horizontal and vertical primary sensitivities of the sensor were 1,479.7 and 1387.8 $\mu VkN^{-1}V^{-1}$, while horizontal and vertical cross sensitivities were 0.64 and 2.85% of the sensor primary sensitivities, respectively. The sensor was used to measure the forces inside the compression chamber of a large square baler in different directions.**


**Keywords**: Calibration, Cross sensitivity, Extended octagonal ring, Force transducer, Large square baler.

## INTRODUCTION

Applied forces to the forage material by baler plunger are exerted to the bale chamber during the baling process. In order to design and optimize the bale chamber structure, having a comprehensive understanding of these forces is necessary. An appropriate sensor is needed to record these compressive forces in different directions. The extended octagonal ring (EOR) is a force transducer through which one is able to measure the forces in different directions independently; therefore, the sensor was designed using two EORs. Ideally, this sensor should measure the forces in different directions independently, but in practice there is always some cross sensitivity in this kind of transducers due to the errors occurring in the machining of the EOR, locating the strain nodes, as well as strain gage installations. It is not possible to eliminate the cross sensitivity, but efforts must be made to reduce this effect during the design, development, and calibration process.

An EOR is developed from circular ring force transducer to give more stability to the transducer. There is no specific analytical equation to calculate the bending moment at the ring section of this kind of transducer; therefore, the equation of extended ring transducer is used in this case as well. The idea of employing EOR in a measurement system was first introduced by Lowen *et al.* (1951). Hoag and Yoerger (1975) derived analytical equations of stress distribution for simple and extended ring transducers at different loading and boundary conditions using strain energy method. They ended up with two equations for the bending moment in the ring section of the extended ring which are used for the moment calculation in the ring section of the EOR. McLaughlin (1996) noticed some errors in one of the

[1] Department of Agricultural Engineering Research, Agricultural Research Center of Fars Province, Zarghan, P. O. Box: 73415-111, Shiraz, Islamic Republic of Iran.
[2] Department of Agricultural and Bioresource Engineering, University of Saskatchewan, 57 Campus Dr., Saskatoon, SK S7N 5A9, CANADA.
*Corresponding author, e-mail: sja925@mail.usask.ca





[ DOR: 20.1001.1.16807073.2009.11.4.11.6 ]

Hoag and Yoerger's equations and corrected them. Godwin (1975) designed an extended octagonal ring transducer to measure the soil reaction forces on soil engaging tools in two directions as well as the moment in the plane of these forces. He reported a good linearity, low cross sensitivities and hysteresis for the transducer. He also found that the practical sensitivities of the strain gages were much greater than the obtained values from analytical equations.

O'Dogherty (1975) designed a transducer to determine the cutting and vertical forces of a sugar beet topping knife using extended octagonal ring. He reported a good linearity, low hysteresis in loading and unloading cycles, and cross sensitivities of 4.1 and 6.5% for cutting and vertical forces, respectively in calibration process of the transducer. Godwin *et al.* (1987) designed three EOR transducers using three different materials with different ratios of ring radius to the ring thickness (r/t). They found that the developed instrumentation systems had sufficient resolution to measure the vertical dynamic behaviour of soil-engaging implements attached to a single pivot hitch.

Godwin *et al.* (1993) designed a dynamometer using two EORs to measure the exerted forces and moments on tillage tools. They used two EORs in back-to-back form the longitudinal axes of which were making angles of 90°. They reported an excellent linearity between applied forces and moments, and bridge output voltage, a small amount of hysteresis effect between loading and unloading calibration curves, as well as a cross sensitivity of less than 4%. However, in one case the reported cross sensitivity was 10.6%. Gu *et al.* (1993) designed and built a transducer to measure the vertical and horizontal forces on the wheels of a quarter scaled model tractor using two EORs. They come up with a regression model for each of the vertical and horizontal primary sensitivities as well as the cross sensitivities. They reported cross sensitivities ranging from around zero to four percent.

O'Dogherty (1996) derived a formula to determine the ring thickness of the EOR transducer while using the data of the designed transducers by the previous researchers. He introduced a graphical procedure for the EOR design based on geometrical parameters of the ring. McLaughlin *et al.* (1998) designed and fabricated a double extended octagonal ring (DEOR) drawbar transducer. They calibrated the transducer employing both uni-axial and tri-axial loading methods. They derived regression models to predict each of the draft, vertical, and side loads, and reported the sensor cross sensitivities of 1.9 and 7.0% for the draft and the vertical loading, respectively. Kheiralla *et al*. (2003) developed a three-point auto hitch dynamometer using EOR transducer. They reported the horizontal and vertical primary sensitivities of 25.19 μstrain $kN^{-1}$ and 25.60 μstrain $kN^{-1}$ for the sensor (77.75% and 89.77% of the computed theoretical sensitivities). Korkut (2003) developed a dynamometer to measure force components during metal cutting in three directions and found that the dynamometer could be reliably used for measuring cutting forces. Jandool Khan *et al*. (2007) designed a bi-axial EOR transducer system to measure tractor-implement forces. They showed that the sensor cross-sensitivity was less than 1.5% for most cases, while the system being best suited when heavy tools were used with a tractor.

The objective of this study was to design, develop, and calibrate an appropriate sensor using EORs to record the forces inside the compression chamber of a large square baler in the longitudinal and vertical directions.

## MATERIALS AND METHODS

### Sensor Design

The sensor was designed using two extended octagonal rings (EOR). The EOR was machined from aluminum 6061-T6 with yield strength of 275 MPa and Young's





[ DOR: 20.1001.1.16807073.2009.11.4.11.6 ]

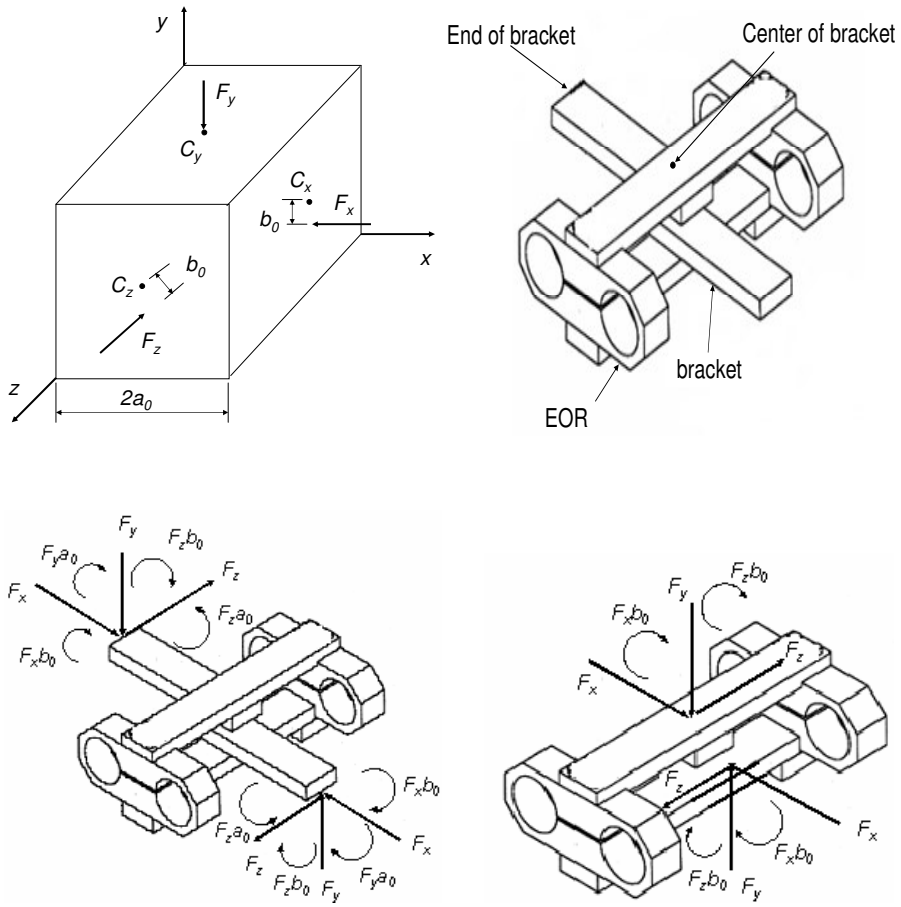


**Figure 1**. Forces transferred from covering plates to the extended octagonal ring (EORs): (a) Forces applied to the cover plates of the sensor; (b) Schematic of the sensor without cover plates; (c) Forces transferred from the covers to the hitch point of sensor, and (d) Forces transferred from the hitch point to the center of braces.

modulus of 70 GPa. A cube of six aluminum plates was used to cover the sensor and provide a suitable sensing area for the applied forces at different directions. Therefore, the outside dimensions of the sensor were: length, 210 mm; height 160 mm; and width, 175 mm. The applied forces on the covering plates of the sensor could be transferred to each of the EORs used in this sensor as shown in Figure 1. Therefore, three forces (Fx, Fy, and Fz) and two moments (My and Mz) are applied to each EOR (Figure 2). Since two sets EOR have been used in this sensor, a half of the applied forces to the covering plates in the x- and y-directions is applied to each EOR. The EOR consists of rigid and flexible parts (Figure 3). The flexible part which is the ring section of the EOR, is used as a sensitive element to bending moment to measure the applied forces by installing strain gages on. These two moments (My and Mz) and orthogonal forces (Fx, Fy, and Fz) apply bending stresses on the "S1" and "S2" sides of the ring section (flexible part) of the sensor (Figure 4). Distribution of stresses created by Fx (horizontal force), Fy (vertical force), and Mz is shown in Figure 4b and the stress distribution created by Fz (lateral force) and My is shown in Figure 4c. In order to sense the strains created by Fx, Fy, and Mz, strain gages must be installed on the face "S2", while strain gages on the face "S1" sense the strain created by Fz and My . The bending moment at different angles of the ring section of this element is calculated from the





[ DOR: 20.1001.1.16807073.2009.11.4.11.6 ]

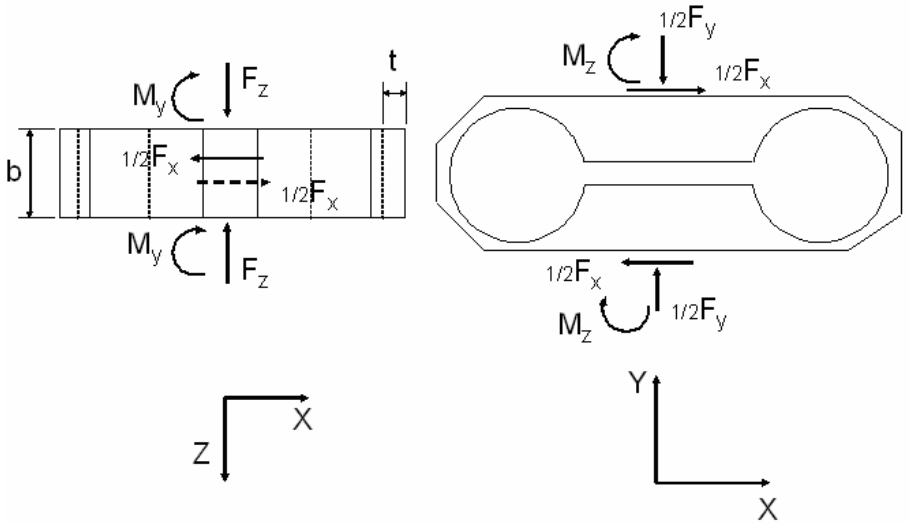


**Figure 2.** Forces transferred from covering plates to the extended octagonal ring in different directions.

$$M_\theta = F_y \frac{R}{2}(\frac{2}{\pi} - \sin\theta) + F_x \frac{R}{2}\cos\theta + M_z \frac{\left[(2 + R\pi/2L) - (2R/L + \pi)\sin\theta\right]}{(8 + R\pi/L + 2L\pi/R)} \quad 0<\theta<\pi \qquad (1)$$

$$M_\theta = F_y \frac{R}{2}(\frac{2}{\pi} + \sin\theta) - F_x \frac{R}{2}\cos\theta - M_z \frac{\left[(2 + R\pi/2L) + (2R/L + \pi)\sin\theta\right]}{(8 + R\pi/L + 2L\pi/R)} \quad \pi<\theta<2\pi \qquad (2)$$

following equation [5, 10]:

where $M_\theta$= Bending moment in ring at angular position θ (N m), ($\theta$= Angle, measured clockwise from the top of ring (radians)), $R$= radius of the ring section (m), $F_x$, $F_y$= Applied forces in the $x$- and $y$-directions (N), $M_z$= Applied external moment (N m) and $L$= One half distance between ring centers (m).

$M_z$ is the moment created by vertical force ($F_y$); therefore, it is the product of $F_y$ by the distance of the acting point of $F_y$ from the center of EOR. Since $F_y$ in this sensor is applied at the center of the EOR, $M_z$ is zero in this case, and Equations (1) and (2) can be written as follows:

$$M_\theta = F_y \frac{R}{2}(\frac{2}{\pi} - \sin\theta) + F_x \frac{R}{2}\cos\theta \qquad (3)$$

$0<\theta<\pi$

$$M_\theta = F_y \frac{R}{2}(\frac{2}{\pi} + \sin\theta) - F_x \frac{R}{2}\cos\theta \qquad (4)$$

$\pi<\theta<2\pi$

In order to measure forces in different directions simultaneously and independently with a minimum of cross sensitivities, proper positions of strain gages must be determined using Equations (3) and (4). For measuring $F_y$, the angle of the location of strain gage must be selected in such a way that the bending moment at that angle is only a function of $F_y$. Therefore, the second term of Equations (3) and (4) should be zero:

$$\pm F_x \frac{R}{2}\cos\theta = 0 \qquad (5)$$

From Equation (5), $\theta$ is obtained to be $\pm 90^\circ$. Therefore, strain gages should be installed at an angle of $\pm 90^\circ$ clockwise from the top point of the ring section to measure $F_y$ with no side effects from $F_x$. For $F_x$ measurement, the first term in Equations (3) and (4) should be equal to zero, therefore:

$$F_y \frac{R}{2}(\frac{2}{\pi} \pm \sin\theta) = 0 \qquad (6)$$





[ DOR: 20.1001.1.16807073.2009.11.4.11.6 ]

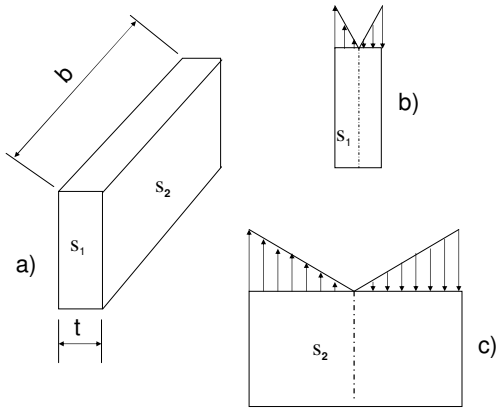


**Figure 4.** Bending stresses applied to the ring section of the sensor: (a) A section of the flexible part (ring section) of the sensor; (b) Bending stress applied by $F_{x \text{ and }} F_y$ on the cross-section of the ring, and (c) Bending stress applied by $F_z$ on the cross-section of the ring .

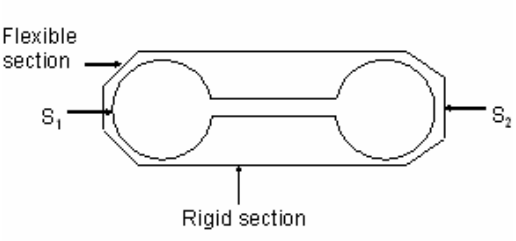


**Figure3**. Flexible and rigid sections of the extended octagonal ring (EOR).

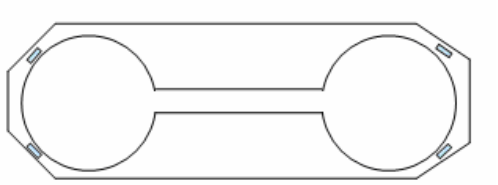

**Figure 5**. Positions of the strain gages on the EOR to record side forces ($F_z$).

From Equation (6), $\theta$ is calculated to be ±39.5° and ±140.5°. So, strain gages should be installed at the angle of ±39.5° and ±140.5° from the top point of the ring section to measure $F_x$ without any side effects from $F_y$. Strain gages installed at these two angles are not affected by $F_z$, because $F_z$ applies shear and torsion at those points which cannot be recorded by these strain gages. In order to measure $F_z$, the strain gages must be installed on the side faces of the ring section (Figure 5).

Based on the above analysis of the strain gage positions, the stress nodes of the EOR (Figure 6) used in this sensor were selected at the positions of $\theta$ = ±39.50°, ±140.5°, and $\theta$ = ±90° for axial and vertical force measurements, respectively. The radius of the ring section of the EOR (R) was taken 25 mm, because it was the smallest required size of the ring for strain gage installation. A ring width of at least 38 mm was needed to attach the horizontal force bracket to the EOR *via* four bolts. The ring center to center distance (2L) was chosen to be 100 mm, and a distance of 50 mm was also required between the two EORs. Based on these dimensions and a preliminary estimation of the maximum plunger pressure, the maximum applied force to the sensor in the *x*- and *y*-directions was found to be about 9 and 5 kN, respectively. Therefore, the horizontal and vertical design loads were considered to be 9 and 5 kN. According to the abovementioned dimensions and design loads, the ring thickness was then determined using Equation (2) along with the following equation [5]:

$$\varepsilon_\theta = \frac{6M_\theta}{Ebt^2} \qquad (7)$$





[ DOR: 20.1001.1.16807073.2009.11.4.11.6 ]

**Table 1.** Dimensions of the extended octagonal ring.

| Parameter | Dimension (mm) |
|---|---|
| t (ring thickness shown in Figure 2) | 6.5 |
| b (ring width shown in Figure 2) | 38 |
| 2L (ring center to center distance shown in Figure 6) | 100 |
| h (shown in Figure 6) | 6 |
| R (ring radius shown in Figure 6) | 25 |

where $b$, $t$= Ring width and thickness (m), $\varepsilon_\theta$ = Strain at angular position θ on the ring which is the allowable strain of aluminum 6061-T6 in this case (m $m^{-1}$), $M_\theta$= Bending moment in the ring at the angular position θ (N m) and $E$= Modulus of elasticity (Pa).

Maximum bending moment of the ring section was calculated using Equations (3) and (4) based on the applied horizontal and vertical forces and the designed angular positions of the mounted strain gages. Then thickness of 6.5 mm was computed for the ring section of the EOR using Equation (7) and having the maximum bending moment ($M_\theta$), the allowable strain for aluminum 6061-T6 (0.0039 m $m^{-1}$), modulus of elasticity of aluminum, and ring width. Once the ring thickness was determined, the ratio of the ring radius to the ring thickness (R/t) was calculated to make sure that the condition for thin ring was satisfied. The designed EOR dimensions are shown in Table 1. Two sets of four strain gages were each installed at the positions of $\theta$= ±39.5°, ±140.5°, and $\theta$= ±90° on the ring section of each EOR. Each set of these strain gages formed a full eheatstone bridge so that there was one horizontal output and one vertical output for each of the EORs (Figure 6). Therefore, the force in the $x$-direction was calculated from the sum of the horizontal outputs of the two EORs, and the force in the y-direction was computed from the sum of the vertical outputs.

## Sensor Calibration

The uni-axial loading calibration was performed by applying forces in the $x$- and y-directions separately to determine the sensor vertical and horizontal primary, secondary, and cross sensitivities. A three directional calibration was also carried out by simultaneously applying forces in the $x$-, $y$-, and $z$-directions to the sensor. Independent forces in the $x$- and $y$-directions were applied using the Wykeham Farrance shear box apparatus while in the $z$-direction, force was applied using a C-clamp. The

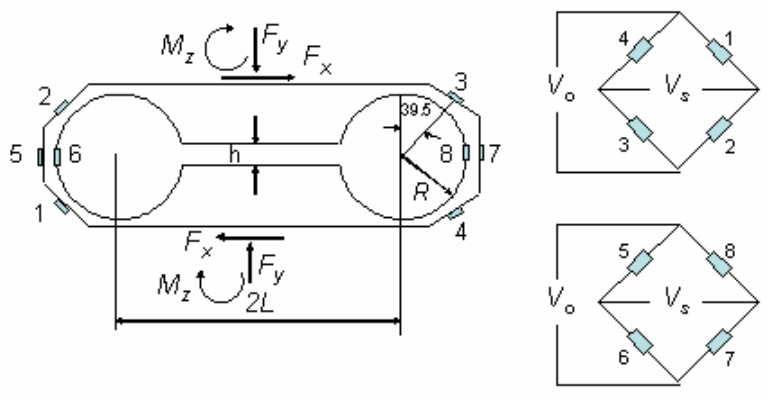


**Figure 6.** Stress nodes and strain gage locations in the extended octagonal ring. Bridge containing gages 1, 2, 3, and 4 is sensitive to $F_x$ while the bridge containing gages 5, 6, 7, and 8 is sensitive to $F_y$.





[ DOR: 20.1001.1.16807073.2009.11.4.11.6 ]

**Table 2**. Cross sensitivities of the sensor resulting from uni-axial calibration.

| Loading axis | Primary sensitivity ($\mu V\ V^{-1}\ kN^{-1}$) | Secondary sensitivity ($\mu V\ V^{-1}\ kN^{-1}$) | Cross sensitivity (%) (Secondary/Primary) |
|---|---|---|---|
| x | 1479.7 | 9.45 | 0.64 |
| y | 1387.8 | 39.55 | 2.85 |

applied force in the *z*-direction was measured by locating a small load cell between the C-clamp and the sensor wall (Figure 7). Four loading along with three unloading points were considered for the three directional calibration.

A data acquisition system including a data logger (PPIO-AI8), a signal conditioner (EXP16), a power supply, and a laptop were used to record the outputs of the sensor at a frequency of 50 Hz. The data of the three directional calibration were used to develop the multiple regression calibration equations to predict each of the forces in the *x*- and *y*-directions. Coefficient of determination ($R^2$) and standard error which is the standard deviation between the experimental data and the data resulting from the model ($\sigma/\sqrt{n}$) were used to evaluate the goodness of the model fitness. The primary, secondary, and the cross sensitivities for each of the horizontal and vertical loadings were also computed using the data of the uni-axial calibration.

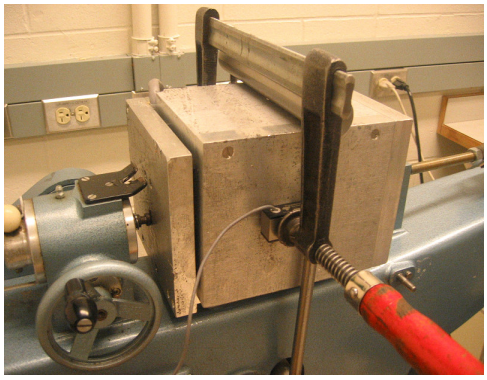

**Figure 7.** Sensor calibration using the Wykeham Farrance shear box apparatus and a C-clamp

## RESULTS AND DISCUSSION

### Sensor Sensitivity

The sensor showed an excellent linearity under the uni-axial vertical and horizontal loading calibration with no hysteresis in the unloading cycle (Figures 8 and 9). Results of the primary, secondary, and the cross sensitivities of the sensor for each of the horizontal and vertical loadings are shown in Table 2. The horizontal and vertical primary sensitivities of the sensor were 1,479.7 and 1,387.8 $\mu V\ V^{-1}\ kN^{-1}$, and cross sensitivities of four arm bridge outputs for the horizontal and vertical loadings were 0.64% and 2.85%, respectively. Godwin (1975) reported horizontal and vertical cross sensitivities of 1.1 and 2.1%, respectively. McLaughlin *et al*. (1998) found a cross sensitivity of 1.9 and 7.0% for the horizontal and the vertical loadings. Gu *et al*. (1993) determined a range of 0 to 4% for the cross sensitivity. Therefore, the horizontal cross sensitivity determined in this study was the lowest as compared to those previously reported, and the vertical cross sensitivity was found to be lower than all the reported vertical cross sensitivities, except that

**Table 3.** Estimated constants of the calibration equations of the sensor.

| Model | $c_x$ | $c_y$ | $c_i$ | $c_0$ |
|---|---|---|---|---|
| $F_x$ | -1214.71 | 7.63 | -13.91 | -450.44 |
| $F_y$ | -15.48 | -1313.99 | -0.53 | -223.41 |





[ DOR: 20.1001.1.16807073.2009.11.4.11.6 ]

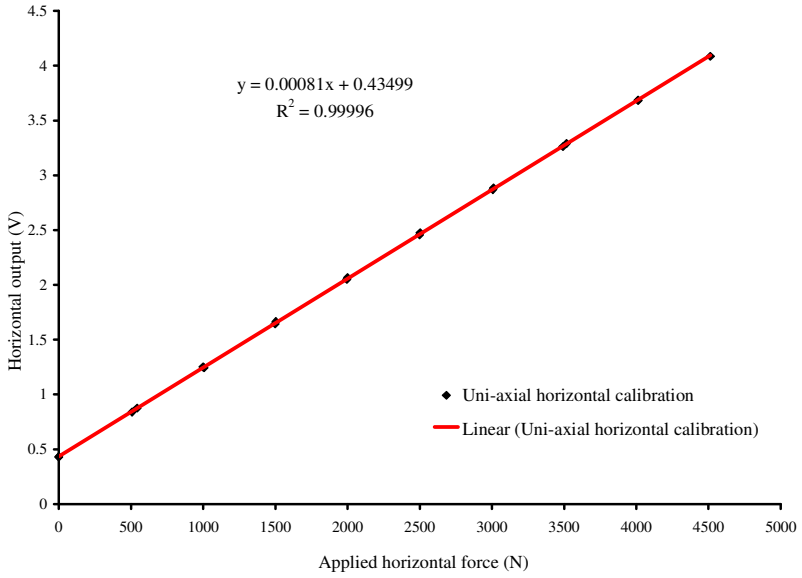


**Figure 8.** Evaluation of horizontal primary sensitivity of sensor.

reported by Godwin (1975).

## Sensor Calibration

The three directional loading calibration data were used to develop the following calibration equations for the forces in the *x*-direction (horizontal force) and the *y*-direction (vertical force) using multiple regression analysis:

$$F_x = c_x V_x + c_y V_y + c_i (V_x V_y) + c_0 , \quad (8)$$

$$F_y = c_y V_y + c_x V_x + c_i (V_x V_y) + c_0 , \quad (9)$$

where $F_x$, $F_y$= Forces in the *x*- and *y*-directions (N), $V_x$, $V_y$= Output of the horizontal and vertical force measurement bridges (v), and $c_x$, $c_y$, $c_i$, $c_0$= Model coefficients. Least square method in multiple regression analysis was employed to validate the developed models and to estimate the model constant coefficients (Table 3).

Results of the multiple regression models for $F_x$ and $F_y$ showed that the best prediction model expressed the forces as a function of primary bridge output, secondary bridge output, as well as the interaction between the primary and secondary outputs. Results also revealed that the lateral force ($F_z$) applied on the sensor had no effect on the output of the horizontal and vertical force measurement bridges. The predicted horizontal and vertical loads versus applied horizontal and vertical loads for the three directional loading calibration are plotted in Figures 10 and 11, respectively. The predicted forces were calculated using the abovementioned multiple regression models. Figure 10 shows that the regression model for the force prediction in the *x*-direction had successfully corrected for the cross sensitivity effects (from forces in other directions) on the force measurement in this direction. The coefficient of determination and the standard error in this case were 0.99 and 28.64 N, respectively (Table 4). A plot of the predicted vertical forces versus applied vertical ones showed that the regression model for the force in the *y*-direction was of the capability to predict the applied forces to the sensor in the *y*-direction ($R^2$= 0.99). However, the random error in this prediction was higher than that in the model predicting force in the *x*-direction. The coefficient of determination and the standard error for the force prediction in the *y*-direction were 0.99 and 86.5 N, respectively (Table 4).





[ DOR: 20.1001.1.16807073.2009.11.4.11.6 ]

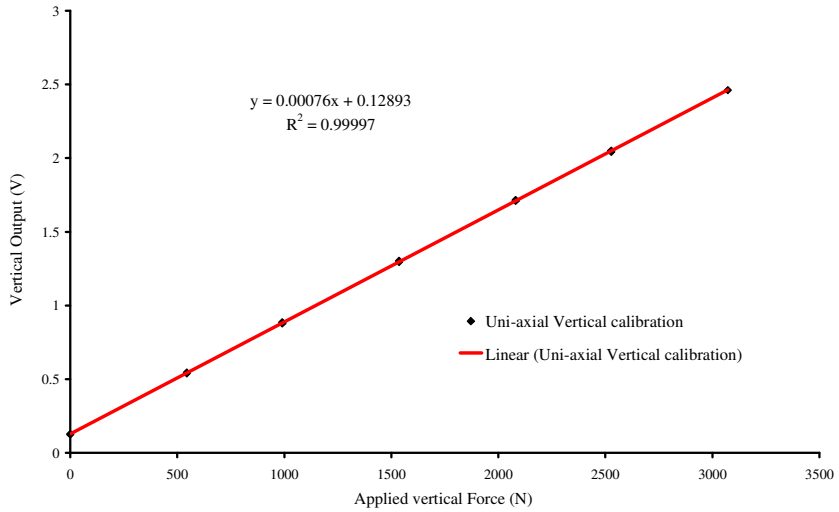


**Figure 9**. Evaluation of vertical primary sensitivity of sensor

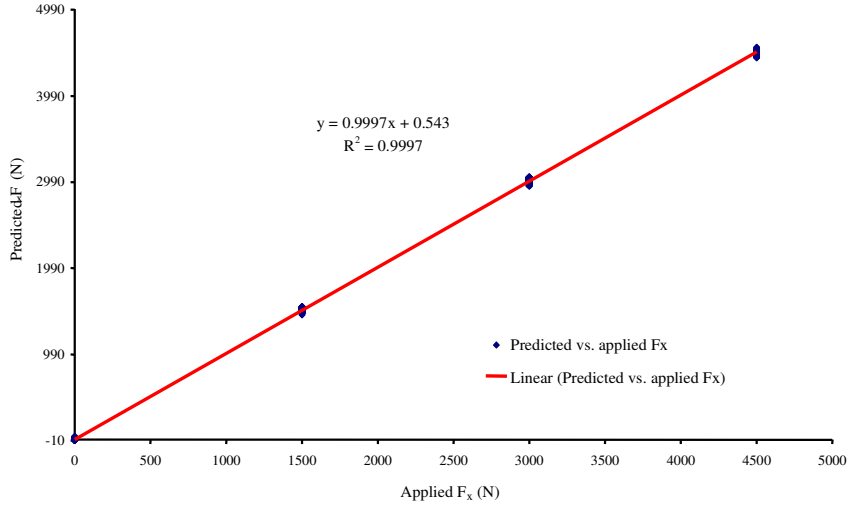


**Figure 10.** Predicted horizontal loads resulting from the developed model in the tri-axial calibration vs. the applied horizontal loads.

Primary sensitivities of the EORs, calculated from the analytical equations and the strain gage bridge theory, were 1,122.4 and 848.8 μV $V^{-1}$ $kN^{-1}$for the horizontal and vertical sensitivities, respectively. These calculated sensitivities were 75.9 and 61.2% of the measured sensitivities (1,479.7 and 1,387.8 μV $V^{-1}$ $kN^{-1}$). These results revealed that the analytical equations used for the EOR design (Equations 2 and 5) underestimated the stress at all positions (θ= ±39.5°, ±140.5°, and θ= ±90°) of the ring section of the EOR.

## Sensor Performance in the Field

The sensor was used to measure the forces inside the compression chamber of a large square baler in different directions when





[ DOR: 20.1001.1.16807073.2009.11.4.11.6 ]

**Table 4.** The coefficient of determination and the standard error of the sensor calibration equations.

| Model | $R^2$ | Standard error (N) |
|---|---|---|
| $F_x$ | 0.99 | 28.64 |
| $F_y$ | 0.99 | 86.5 |

**Table 5.** Error of the extended octagonal ring transducer in measuring plunger force when barley straw baled

| Measurement method | Plunger force (kN) | Error (%) |
|---|---|---|
| EOR transducer | 9 | 5.26 |
| Strain gage | 8.55 | |

barley as well as wheat straw were being baled. The sensor was placed inside the bale by creating an opening at the center of the bale cross section (Figure 12). The sensor was able to record the forces inside the bale chamber at different distances from the plunger when it was moving from the plunger head to the end of bale chamber along and together with the bale. To evaluate the accuracy of the sensor, a set of four strain gages (EA-06-500BL-350, Microsoft Measurements, Raleigh, North Carolina) were mounted each on the each arm of the plunger to measure the forces exerted on the plunger (Figure 13).

Results of force measurement inside the compression chamber in the x-direction were close to those obtained for the baler plunger maximum force when strain gages installed on the plunger arms. The error for the force measurement when using the sensor for barley straw was about 5.3% (Table 5). A sample of the recorded forces in the x-direction inside the bale chamber of a large square baler for baling barley straw is shown in Figure 14. As shown in the figure, bale chamber force was varied exponentially from the plunger (x =0 cm) to the end of bale chamber (x= 240 cm) so that the

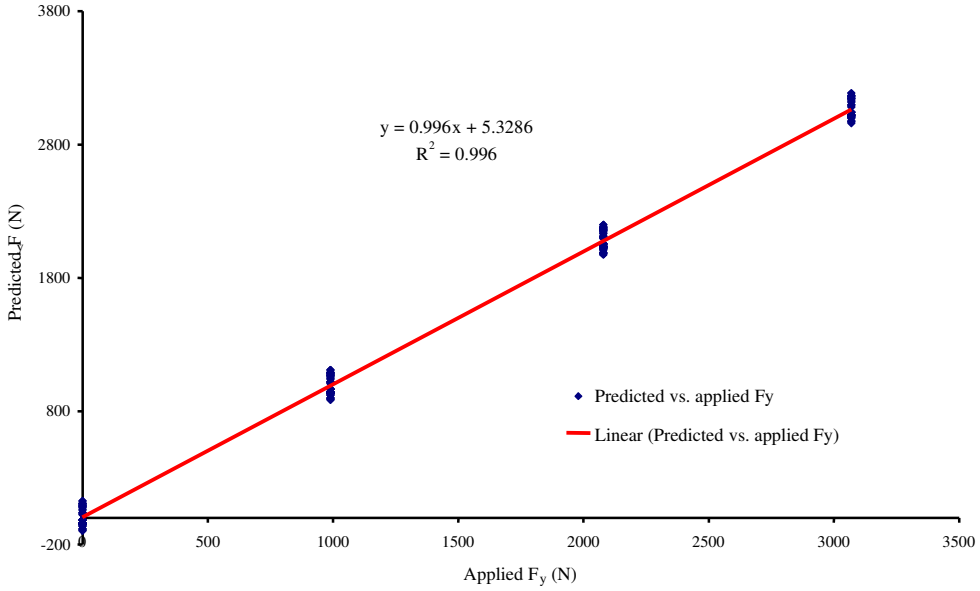


**Figure 11.** Predicted vertical loads resulting from the developed model in the tri-axial calibration vs. the applied vertical loads.





[ DOR: 20.1001.1.16807073.2009.11.4.11.6 ]

**Figure 12**. extended octagonal ring sensor placed inside the bale.

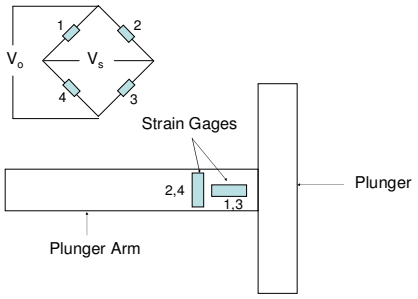


**Figure 13.** Arrangement of strain gages on the plunger arm and Wheatstone bridge.

maximum force was recorded on the plunger head and the minimum recorded at the end of the bale chamber. According to the theoretical analysis given in materials and methods, forces in the z-direction could not be recorded by the strain gages mounted on this sensor. Therefore, this sensor could only record the forces in the x- and y-directions. In order to make the sensor a perfect tri-axial force transducer, a set of stain gages must be mounted on the side faces of the ring section of the EOR (Figure 5) to be able to record Fz in addition to Fx and Fy.

## CONCLUSIONS

A sensor was designed using an extended octagonal ring (EOR) and was calibrated uni-axially as well as tri-axially. The sensor exhibited excellent linearity and low cross sensitivities. Horizontal and vertical primary sensitivities of the sensor were 1,479.7 and 1,387.8 $\mu V\ V^{-1}\ kN^{-1}$, and the horizontal and vertical cross sensitivities were 0.64 and 2.85% of the sensor primary sensitivities, respectively. Primary sensitivities of the

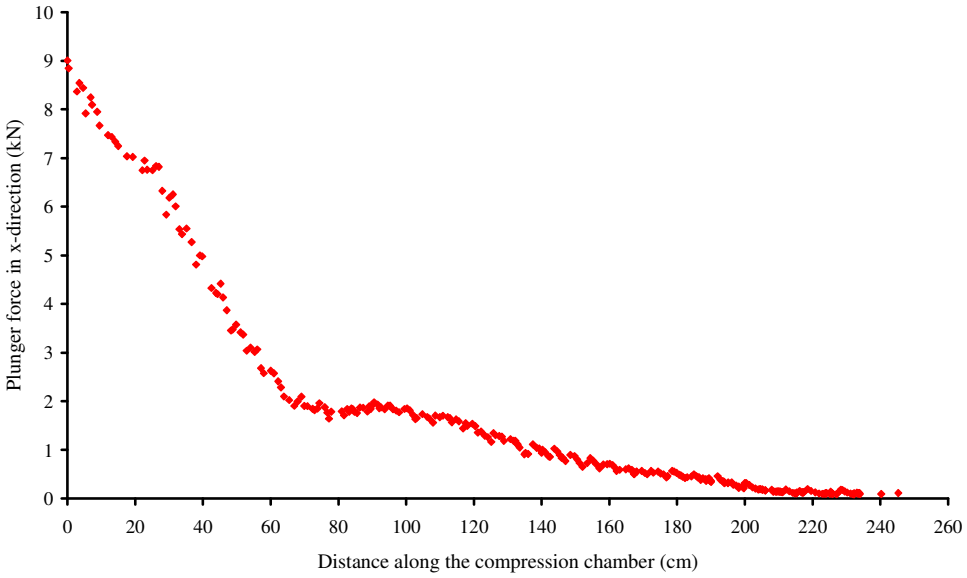


**Figure 14.** Plunger forces recorded by the designed transducer in the x-direction inside the bale chamber of a large square baler for baling barley straw.





[ DOR: 20.1001.1.16807073.2009.11.4.11.6 ]

EORs calculated from the analytical equations and from the strain gage bridge theory were 1,122.4 and 848.8 $\mu V\ V^{-1}\ kN^{-1}$ for the horizontal and the vertical sensitivities, respectively. These calculated sensitivities were 75.9 and 61.2% of the measured ones (1,479.7 and 1,387.8 $\mu V\ V^{-1}\ kN^{-1}$). Therefore, the results reveal that the analytical equations used for the EOR design (Equations 2 and 5) underestimated the stresses at all positions ($\theta = \pm 39.5^{\circ}$, $\pm 140.5^{\circ}$, and $\theta = \pm 90^{\circ}$) of the ring section of the EOR. Results of the force measurement inside the bale compression chamber in the *x*-direction were close to the results obtained for the baler plunger maximum force recorded when strain gages installed on the plunger arms. As for barley straw, the error for the force measurement, using the sensor in the *x*-direction was approximately 5.3%.

## ACKNOWLEDGEMENTS

The authors would like to acknowledge the financial support extended by the CNH Company. The valuable help from W. Morley during the machining of the EOR and instrumentation set up is also appreciated.

## REFERENCES

1. Godwin, R. J. 1975. An Extended Octagonal Ring Transducer for Use in Tillage Studies. *J. Agric. Eng. Res.,* **20**: 347-352.
2. Godwin, R. J., Magalhaes, P. S. G., Miller, S. M. and Fry, R. K. 1987. Instrumentation to Study the Force System and Vertical Dynamic Behaviour of Soil-engaging Implements. *J. Agric. Eng. Res.,* **36**: 301-310.
3. Godwin, R. J., Reynols, A. J., O'Dogherty, M. J. and Al-Ghazal, A. A. 1993. A Triaxial Dynamometer for Force and Moment Measurements on Tillage Implements. *J. Agric. Eng. Res.,* **55**: 189-205.
4. Gu, Y., Kushwaha, R. L. and Zoerb, G. C. 1993. Cross Sensitivity Analysis of Extended Octagonal Ring Transducer. *Trans. ASAE*, **36(6):** 1967-1972.
5. Hoag, D. L. and Yoerger, R. R. 1975. Analysis and Design of Load Rings. *Trans. ASAE,* **19**: 995-1000.
6. Khan, J., Godwin, R. J., Kilgour, J. and Blackmore, B. S. 2007. Design and Calibration of a Bi-axial Extended Octagonal Ring Transducer System for the Measurement of Tractor-implement Forces. *J. Eng. Appl. Sci.,* **2(1):** 16-20.
7. Kheiralla, A.F., Yahya, A., Zohadie, M. and Ishak, W. 2003. Design and Development of a Three-point Auto Hitch Dynamometer for an Agricultural Tractor. *AJSTD*, **20(3 and 4):** 271-288.
8. Korkut, I. 2003. A Dynamometer Design and Its Construction for Milling Operation. *Materials and Design*, **24(8):** 631-637.
9. Lowen, E. G., Marshall, E. R. and Shaw, M. C. 1951. Electric Strain Gauge Tool Dynamometers. *Proc. Soc. Exp. Stress Analysis*, **8(2):** 1-16.
10. McLaughlin, N. B. 1996. Correction of an Error in Equations for Extended Ring Transducers. *Trans. ASAE,* **39(2):** 443-444.
11. McLaughlin, N. B., Tessier, S. and Guilbert, A. 1998. Improved Double Extended Octagonal Ring Drawbar Transducer for 3-D Measurement. *Can. Agric. Eng.,* **40**: 257-264.
12. O'Dogherty, M. J. 1975. A Dynamometer to Measure the Forces on a Sugar Beet Topping Knife. **20**: 339-345.
13. O'Dogherty, M. J. 1996. The Design of Octagonal Ring Dynamometer. *J. Agric. Eng. Res.,* **63**: 9-18.





[ DOR: 20.1001.1.16807073.2009.11.4.11.6 ]

# حسگر سنجش نیرو با استفاده از رینگ هشت وجهی بسط یافته برای محفظه تراکم بیلر مکعبی بزرگ

**ص. افضلی نیا و م. روبرژ**

## چکیده

حسگر اندازه گیری نیروهای داخل محفظه تراکم بیلر مکعبی بزرگ با استفاده از رینگ های هشت وجهی بسط یافته ساخته شد. این حسگر با اعمال نیرو در جهات مختلف به طور همزمان و مستقل از یکدیگر کالیبره گردید. نتایج کالیبراسیون نشان داد که رابطه بین ورودی وخروجی حسگر کاملا خطی است و حساسیت متقابل اندکی بین خروجی های افقی و عمودی حسگر وجود دارد. حساسیتهای اولیه افقی و عمودی به ترتیب ۱۴۷۹/۷ و۱۳۸۷/۸ میکرو ولت بر ولت-کیلونیوتن و حساسیتهای متقابل افقی و عمودی به ترتیب ۰/۶۴ و۲/۸۵ در صد حساسیت اولیه حسگر بودند. این حسگر جهت اندازه گیری نیروهای داخل محفظه تراکم یک دستگاه بیلر مکعبی بزرگ در جهات مختلف مورد استفاده قرار گرفت.



[ DOR: 20.1001.1.16807073.2009.11.4.11.6 ]